College of Engineering

ISSN: 1813-162X (Print) ; 2312-7589 (Online)

Tikrit Journal of Engineering Sciences

available online at: http://www.tj-es.com

TJES
Tikrit Journal of Engineering Sciences

Effect of Fluidized Bed Particle Size on Heat Transfer Coefficient at Different Operating Conditions

Ehsan Fadhil Abbas*

Sarah Burhan Izat

Refrigeration and Air Conditioning Department
Technical College/ Kirkuk
Northern Technical University
Iraq

***Keywords*:**

Fluidized bed
heat transfer coefficient
particle size

ARTICLE INFO

Article history:

Received 19 February 2018
Accepted 29 July 2018
Available online 01 December 2018

Tikrit Journal of Engineering Sciences Tikrit Journal of Engineering Sciences Tikrit Journal of Engineering Sciences Tikrit Journal of

A B S T R A C T

The aim of this study is to investigate the effect of gas flow velocity, size of sand particles, and the distance between tubes immersed in a fluidized bed on heat transfer coefficient. Experimental tests were conducted on a bundle of copper tubes of (12.5 mm) diameter and (320 mm) length arranged in a matrix (17×9) and immersed in a fluidized bed inside a plastic container. One of the tubes was used as a hot tube with a capacity of (122 W). (25 kg) of sand with three different diameters of sand particles (0.15, 0.3 and 0.6 mm) was used in these tests at ten speeds for gas flow (from 0.16 m/s to 0.516 m/s). The results showed a significant inverse effect of fluidized bed particles diameter on the heat transfer coefficient. Accordingly, the heat transfer coefficient for (0.15mm) diameter sand was found to be higher than that of (0.3 mm) and (0.6 mm) sand by about (3.124) and (6.868) times respectively, in all tests. The results showed good agreement with results from other studies conducted under the same conditions but with different sand particle size.

© 2018 TJES, College of Engineering, Tikrit University

DOI: http://dx.doi.org/10.25130/tjes.25.4.05

تأثير حجم جسيمات الطبقة المميعة على معامل انتقال الحرارة عند ظروف تشغيلية مختلفة

الخلاصة

تهدف هذه الدراسة الى التحقق من تأثير كل من سرعة الغاز، حجم جسيمات الرمل والمسافة بين الاعمدة المغمورة في الطبقة المميعة على معامل انتقال الحرارة. حيث اجريت اختبارات تجريبية على حزمة من الانابيب نحاسية بقطر (12.5) ملم وطول (320) ملم ورتبت على شكل مصفوفة (17×9) مغمورة في الطبقة المميعة داخل حاوية بلاستيكية. استخدمت احدى الانابيب كمصدر للحرارة بسعة (122) واط. استخدمت ثلاثة قياسات لجسيمات الرمل (0.15، 0.3 و0.6) ملم وبعشر سرع تراوحت من (0.16 الى 0.516) م/ ثا. اظهرت النتائج بأن تأثير عكسي كبير لقطر جسيمات الرمل في الطبقة المميعة على معامل انتقال الحرارة. وفقا" لذلك، فان معامل انتقال الحرارة عند الرمل بقطر (0.15) ملم الذي حصل عليه كانت اعلى عما حصل عليه عند (0.3) ملم و (0.6) ملم بحوالي (3.124) و (6.868) مرة على التوالي في جميع الاختبارات. تظهر النتائج بانها توافق بشكل جيد مع نتائج لدراسات اخري اجريت تحت نفس الظروف ولكن مع قياسات الرمل مختلفة.

1. INTRODUCTION

Fluidized beds are widely used in industrial and physical processes such as coating, drying, mixing, granulating, heating, cooling and many other applications, due to the mixing ability of the fluidized bed. It is also used for chemical processes such as catalyst cracking, reactor composition, olyphine polymerization, silicon production, liquefied coke, flexible coke, and waste coal combustion (biomass) [1]. The earliest utilization of the fluidization technique was in gas production by the German chemist Fritz Winkler in 1922. In addition to gas production, this technique has been successfully utilized in thermal cracking processes in the United States in 1942 [2]. Nowadays, the fluidization technique is used widely in all industries such as oil and other industries, and is adopted intensively in the chemical industry as a viable and applicable technique since 1970. Furthermore, it is adopted as an auxiliary technique to help in combustion processes and gas production (gasification). In order to develop and benefit from this technique by improving the thermal performance of heat exchangers, many theoretical and

* *Corresponding author: E-mail* : ehsanfadhil@gmail.com

Nomenclatures

A	surface area, (m^2)
D_t	tube diameter, (m)
d_p	sand particle diameter, (m)
G	gravitational acceleration, (9.81 m^2/sec)
$\bar{h}$	average heat transfer coefficient, ($W/m^2.{}^oC$)
h	convection heat transfer coefficient, ($W/m^2.{}^oC$)
H	pressure difference, (mm Hg)
HT	hot tube
L	tube length, (m)
k_g	thermal conductivity of gas (W/m. ^oC)
Q	heat transfer rate, (W)
S_L	longitudinal distance, (m)
S_T	lateral distance, (m)
T_b	local bed temperature, (^oC)
$\overline{T_b}$	average bed temperature, (^oC)
T_W	wall temperature, (^oC
$\overline{T_w}$	average wall temperature, (^oC)
T_f	film temperature, (^oC)
U	gas velocity, (m/sec)
ϑ_g	kinematic viscosity of gas, (m^2/sec)
φ	any property of air flow
$X_1..X_2$	hot tube's location

Dimensionless Group

Re_t	tube Reynolds number
Re_p	particle Reynolds number
$\overline{Nu_t}$	average tube Nusselt number
$\overline{Nu_p}$	average particle Nusselt number

experimental studies have been conducted by different researchers in this field. Some of these studies will be reviewed in this study. Wu et al. [3] conducted an experimental study to calculate the local and hydrodynamic heat transfer in a circulating fluidized bed. They used a fluidization column of 152 mm diameter and 9.3 m length, while the sand particle's (Ottawa sand) diameter was 171 μm specify the types of circulation. The study results revealed that the voidage has a significant effect on the heat transfer within the circulating fluidized bed. Furthermore, the density of particles has an important impact on the heat transfer coefficient as it related directly to the void's concentration during fluidization. Masoumifard et al. [4] introduced an empirical relationship for the heat transfer between the horizontal tube and the fluidized bed (gas-solid). In their study, a hot horizontal tube of 8 mm diameter was immersed in a fluidized bed. Three types of fluidized beds were used with different sand particle diameters of (280, 490 and 750) µm, using air as the fluidizing fluid. The results showed that the heat transfer coefficient increases with decreases in the size of sand particles, while increases and then slightly decrease with increases in air flow velocity to the highest value. The effect of sensors location on the heat transfer coefficient is found to be slight. Stefanova et al. [5] conducted an experimental study to calculate the heat transfer from a tube immersed in a fluidized bed consisting of particles in the region from a transition fluidization flow to a turbulent fluidization flow. The tests were conducted in a glass column of 0.29 m diameter and 4.5 m length to measure the heat transfer in the fluidized bed using fluid cracking catalytic (FCC) of 70 μm diameter. The results showed that the amount of heat transfer increases with increases in gas velocity. Additionally, the increase in the frequency of particles striking the wall has led to an increase in the heat transfer coefficient without any noticeable effect on the depth of the fluidized bed. However, during turbulent flow, there was a noticeable effect of 25% between the first fluidized bed (1.2 m) and the second fluidized bed (0.8 m). Habeeb and Al-Turaihi [6] experimentally investigated the behavior of gas - solid flow in the tubes of circular shape fluidized beds in 2 phases (air and sand) at steady and unsteady states in the vertical tube. Three different diameters of sand particles were used (300, 550 and 800 μm) as a fluidizing media at different air velocities ranging from 1.4 m/s to 2.1 m/s. The tests were conducted using a horizontal electrical heater with a diameter of 3.175 cm and three capacities (100, 140 and 180 W). The results were analysed using computational fluid dynamics (CFD) software (FLUENT) to determine the flow behavior and temperature distribution along the fluidized bed depth. The results showed that the temperature distribution along the column decreases with increases in particle size, and increases with increases in heat flow. On the other hand, Makkawi [7] experimentally measuring the heat transfer in a circulating fluidized-bed (CFB) using a fluidization column of 5.2 cm diameter and 163cm length with maximum flow rate of 1300 lit/min. Two diameters of glass particles were used in the study (235 μm and 700 μm) with a mass of 10 kg. The results showed that the glass particles were stable during movement in small spaces, then quickly gained heat and became unstable. Furthermore, the heat transfer coefficient increases with decreases in particle diameter. Chourasia and Alappat [8] experimentally investigated the effects of operation time on the attrition and size distribution of sand particles in a circulating fluidized bed. The experiments were performed on the sand size ranging from (1 to 2) mm at ambient condition and superficial air velocity ranging from (7.13 to 9.16) m/s. It has been observed that the coefficient of uniformity and coefficient of curvature showed increasing patterns. It specifies that particles of different size ranges and fines were formed due to attrition of particles.

The aim of this study is to experimentally investigate the effect of fluidized bed sand particle diameters on the heat transfer coefficient under different operating conditions. These conditions include the hot tube's location inside the first row of the tubes bundle and the velocity of the entering gas to the fluidized bed. Three fluidized bed's sand particle diameters were used in these tests (0.15, 0.3 and 0.6 mm) to calculate the Nusselt number for the sand particles and the tube.

2. EXPERIMENTATION

2.1. Experimental Setup

The test rig shown in Fig. 1 was built to conduct the experiments. It consisted of 6 mm thick plastic container with dimensions of 30×60 cm and 100 cm installed on a structure of V-type iron bars (size 25 mm). A bundle of copper tubes of 12.5 mm diameter and 32 cm length was arranged inside the bed in a matrix of 9×17. One of these tubes which were used as a hot tube contained an electrical heater of 122 W capacities shown in Fig. 2. To ensure uniform air flow inside the container, a conical box had been manufactured and fixed to the bottom of the container. The conical box contained:

a- A layer of commercial sponge to prevent the leakage of sand particles from the container to the box.

b- Paper filters (to prevent the entry of sand particles into the air blower).

c- An air distributor made of a wooden board with dimensions of 56×26 cm and 2cm thickness which contain 263 holes of 10 mm diameter to ensure equal air distribution within the whole fluidized bed.

d- Four channels to transmit air into the air distribution plate (to give a steady flow of air to the fluidization region to prevent unstable flow (air jets)).

Three types of sand were used in the tests after washing, drying and sifting depending on the diameters required. Two sensors for measuring pressure difference were used; one on the orifice disk to measure the air velocity, and the other inside the fluidized bed to measure the pressure difference within the bed. A data logger with 22 channels was used to collect temperature data through K-type thermocouples distributed as follows:

1. Five thermocouples fixed on the hot tube (HT).
2. Fifteen thermocouples distributed within the fluidized bed in different places.
3. Two thermocouples fixed on the entry and exit of air into the fluidized bed.

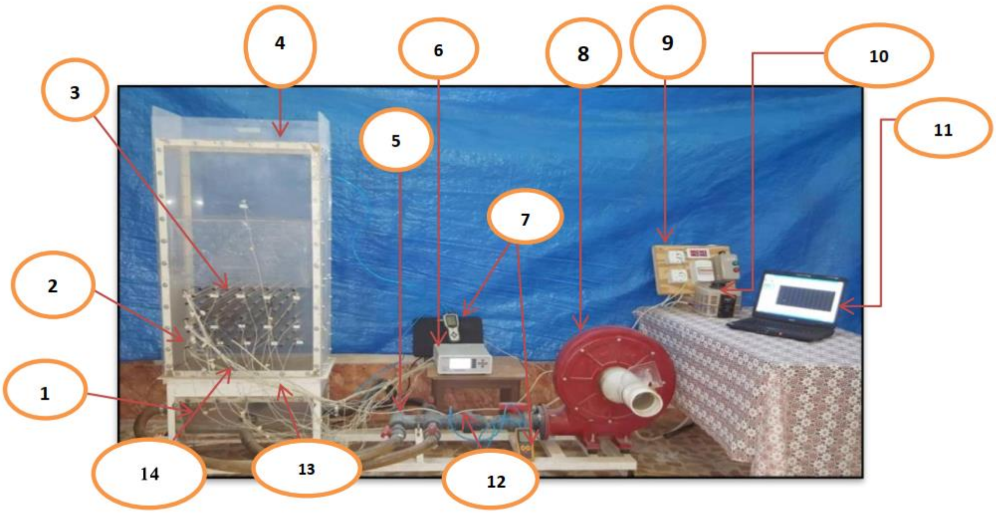

1	Conical box	6	Temperature data logger	11	Computer
2	Hot tube	7	Pressure difference measurement devices	12	Orifice
3	Copper tube	8	Centrifugal blower	13	Air distributor and filter
4	Plastic container	9	Electricity panel	14	Thermocouples
5	Pipe system	10	Power supply		

Fig. 1. Experimental test rig.

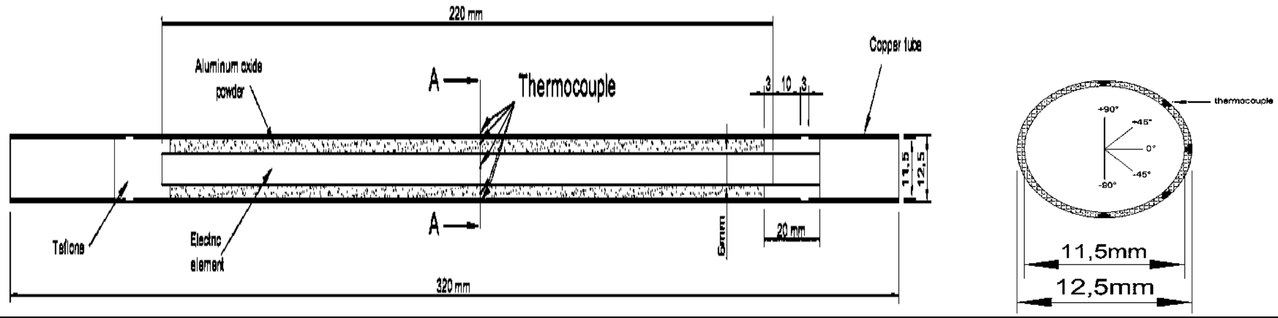

(a) (b)

Fig. 2. Schematic of a hot tube (a) Details of the hot tube and (b) Thermocouples location.

2.2. Experimental Procedures

1. Install the container in the test rig tightly to prevent the leaking of sand particles into the box or out of the container, and then insert the tubes in the desired place and fix it on the container wall.
2. Insert the hot tube in location (X_1) as shown in Fig. 3.
3. Fill the plastic container with sand (0.15 mm diameter) to the height of the first row of tubes which requires 25 kg of sand.
4. Connect the electrical power to the hot tube using the power supply, and wait for a period of time until the heater surface reaches a temperature of 200 °C.
5. Run the air blower, with the main valve and gate installed at the air entrance to the blower closed at the beginning.
6. Run the air blower and control the air flow velocity from the main valve and gate installed at the air entrance. Choose four speeds for each particle diameter as follows:

a- 0.16 m/s, 0.2 m/s, 0.221 m/s and 0.254 m/s for sand with 0.15 mm particle diameter.
b- 0.221 m/s, 0.254 m/s, 0.3 m/s and 0.338 m/s for sand with 0.3 mm particle diameter.
c- 0.349 m/s, 0.423 m/s, 0.48 m/s and 0.516 m/s for sand with 0.6 mm particle diameter.

A period of 15 minutes is allocated for the air flow to reach a steady state through the fluidized bed.

1. Repeat procedures 1 to 6 in tests on the location of heaters from tube X_2 to the last tube X_5.
2. After the completion of tests on the first sand sample (15 mm), change to the second sample (0.3 mm) and third sample (0.6 mm) respectively by following the above procedures for each measurement.

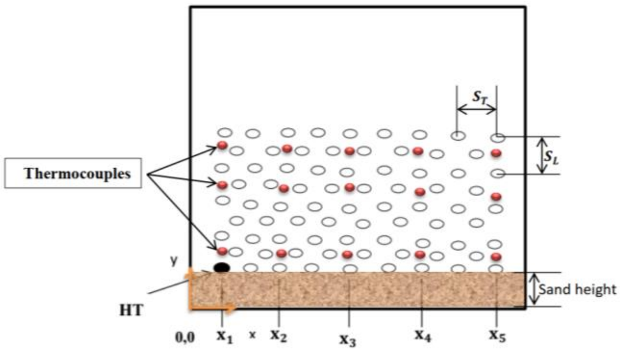

Fig. 3. Simple diagram for the locations of hot tube in the plastic container.

2.3. Calculation Approach

The Nusselt number (*Nu*) and Reynolds number (*Re*) were calculated using the results obtained from tests conducted on the three samples of sand as follows:

1- To calculate the local value of h at each angle of the outer surface of the hot tube, the Newton's law of cooling is used as:

$$h = \frac{Q}{A\,(T_w - T_b)} \tag{1}$$

where,

$$A = \pi\, D_t\, L \tag{2}$$

The average of convective heat transfer coefficient is calculated using the average of the local values of the five angles on the surface of the hot tube from the mathematical relation in Eq. (3).

$$\bar{h} = \frac{\sum_{j=1}^{j=5} h_j}{5} \tag{3}$$

The air properties (k, ϑ) are found at (T_f) using the air physical properties table at atmospheric pressure [9]:

$$T_f = \left[\frac{\overline{T_w} + \overline{T_b}}{2}\right] + 273 \tag{4}$$

where

$$\overline{T_w} = \frac{\sum_1^5 T_w}{5} \tag{5}$$

and

$$\overline{T_b} = \frac{\sum_{i=1}^{i=15} T_{b,i}}{15} \tag{6}$$

Then, the Nusselt number for the tube and sand particles (Nu_t & Nu_p) are calculated from the following relations [10]:

$$\overline{Nu_t} = \frac{\bar{h}\, D_t}{k_g} \tag{7}$$

$$\overline{Nu_p} = \frac{\bar{h}\, d_p}{k_g} \tag{8}$$

2- The Reynolds number for the tube and sand particles (Re_t & Re_p) are calculated as follows [10]:

$$Re_t = \frac{U\, D_t}{\vartheta_g} \tag{9}$$

$$Re_p = \frac{U\, d_p}{\vartheta_g} \tag{10}$$

To find gas velocity, Bernoulli's law is used to convert the pressure difference into velocity [11]:

$$U = \sqrt{2gH} \tag{11}$$

2.4. Experimental Error Analysis

The results should be tested for uncertainty using the experimental error method because they contain three types of error, as instrument calibration, bias errors, and random errors [13]. The following is a summary of the uncertainty of the use of measuring devices and experimental data.

1. Measurements uncertainty

The bias error is calculated from [12] for the following measuring instruments used in this study.

$$B = \pm\left[\sqrt{\left(\frac{1}{2} \times Resolution\right)^2 + (Accuracy)^2}\right]^{1/2} \tag{12}$$

2. Dimension uncertainty
   - Hydraulic diameter ±0.29%.
   - Outer surface area ±0.55%.
3. The relative pressure drop uncertainty ±0.653%.
4. Uncertainty estimation of air properties.

The uncertainty estimation of these properties has been calculated based on the following relation [12]:

$$U_\varphi = \pm\frac{1}{2}\left|\varphi_{\left(\frac{\bar{T}_{in}+\bar{T}_w}{2}\right)_{max}} - \varphi_{\left(\frac{\bar{T}_{in}+\bar{T}_w}{2}\right)_{min}}\right| \tag{13}$$

Table 2
Measuring devices uncertainty.

Device	Resolution	Accuracy	Bias error (B)
Caliper	0.01 mm	±0.02 mm	±0.0206 mm
Power meter	0.01 W	(0.01±5)W	±0.0112 W
Differential pressure meter	0.04 psi	±0.06 psi	±0.0632 psi
Temperature data logger	0.1 ℃	0.2 ℃	±0.206 ℃

Table 3
Uncertainty estimation of air properties.

Air properties	Uncertainty ratio (%)
Density	±1.232
Specific heat	±0.094
Thermal conductivity	±1.186
Dynamic viscosity	± 0.939
Prandtl number	± 2.663

1. Uncertainty for Reynolds number ± 1.707%.
2. Uncertainty for Nusselt number ± 3.163%.
3. Uncertainty for heat transfer coefficient ± 3.391%.

3. RESATLS AND DISCUSSION

The value of heat transfer coefficient (*h*) between the fluidized bed and the hot tube immersed in it was affected by the bubble destroying behavior and the movement of the fluidized bed particles due to the gas flowing through the bed [13]. The effect of individual behavior of thermocouples locations which were installed on the hot tube was determined at different gas velocities. Then, the average of the Nusselt number was calculated for both the tube and sand particles from the experimental data using Eqs. (1)-(7). A graph is used to represent the relation between the average $\overline{Nu}$ and R_e for the tube and particles at different gas velocities. Figs. 4-6 illustrate the effect of each of the hot tube position and Reynolds number on the tube's average Nusselt number for sand samples 0.15, 0.3, and 0.6 mm. Figs. 7- 9 show the effect of each of the hot tube position and Reynolds number on the Nusselt number for sand particle samples 0.15, 0.3, and 0.6 mm. As observed from these figures, in general, $\overline{Nu}$ increases with increases in R_e. For the influence of the hot tube location, it is clearly obvious for each case, where the maximum value of $\overline{Nu}$ was observed for the 0.15mm sand sample at location X_1. Furthermore, the maximum value of $\overline{Nu}$ at Re=200 was about 235, an increase by 15% compared to the other locations (X_3 and X_5) as shown in Fig. 4. As for the 0.3 mm sand sample, it is observed in Fig. 5 that the $\overline{Nu}$ values are lower than that of the previous sand sample, where the maximum values at locations X_2 and X_3 did not exceed 25% of the achieved value in the previous sample. It was also observed in Fig. 4 that the values of $\overline{Nu_t}$ at these two locations were significantly influenced by the increase in *Re* compared to locations X_1, X_4 and X_5 where there was less effect of *Re* on $\overline{Nu_t}$. However, when the 0.6 mm sand sample was used, the tests results showed that the value of $\overline{Nu_t}$ in this case is less than the calculated value from the previous sand samples in all the locations of the hot tube. The maximum value of $\overline{Nu_t}$ calculated at the location of X_2 was about 35 to 37 for a range of *Re* of 180 to 300 as shown in Fig. 6. This value of $\overline{Nu_t}$ is lower than the maximum value of $\overline{Nu_t}$ obtained for the 0.15 mm sand sample by 5 times. Although the ranges of *Re* for the 0.15 mm sand sample are less than the other sand samples, the value of $\overline{Nu_t}$ is higher. The analysis of the tests results based on the molecular diameter of sand are illustrated in Figs. 7-9 for sand sizes 0.15, 0.3, and 0.6 mm respectively. It is observed from these figures that the values of Nu_p is much lower compared to that of $\overline{Nu_t}$ and did not exceed more than 3 in its best case. It was observed in the 0.15 mm sand sample that the maximum value of Nu_p had ranged between 2.5 to 3 at location X_1, while at the other locations, there is a significant effect of *Re* on the changing values of $\overline{Nu_t}$ as shown in Fig. 7. On the other hand, Fig. 8 shows the test results for the 0.3 mm sand sample. It is obvious that the obtained values for Nu_p are much lower compared to that of the 0.15 mm sand sample with a maximum reduction of 30%. Fig. 9 shows the test results for the 0.6 mm sand sample. It is obvious that the obtained values for Nu_p are lower than the corresponding

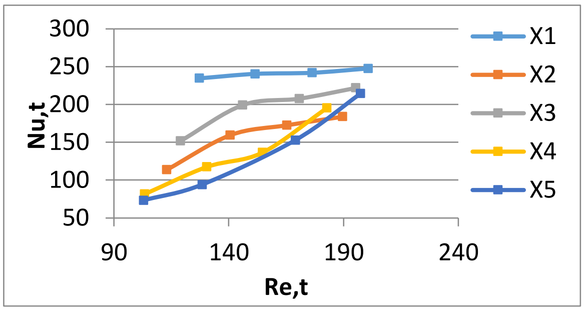

Fig. 4. Effect of Reynolds number on the tube Nusselt number for the sand samples 0.15 m.

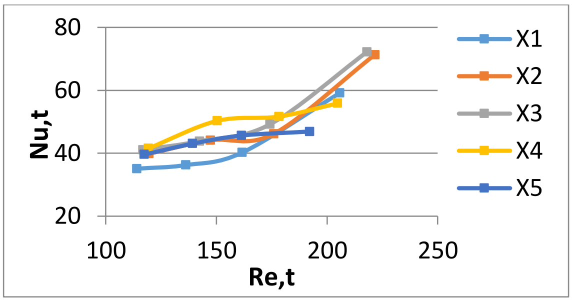

Fig. 5. Effect of Reynolds number on the tube Nusselt number for the sand samples 0.3 mm.

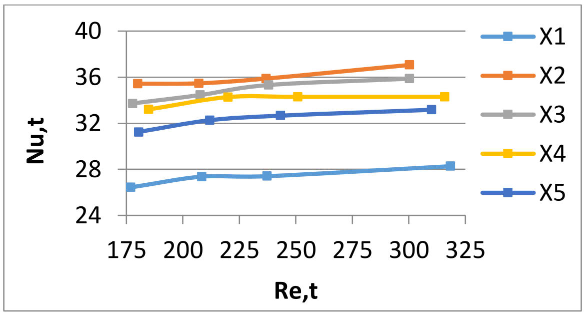

Fig. 6. Effect of Reynolds number on the tube Nusselt number for the sand samples 0.6 mm.

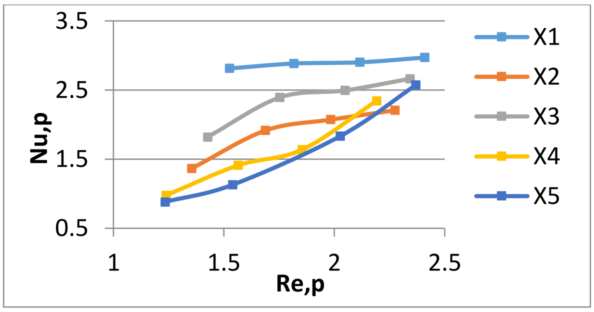

Fig. 7. Effect of Reynolds number on the particles Nusselt number for the sand samples 0.15mm

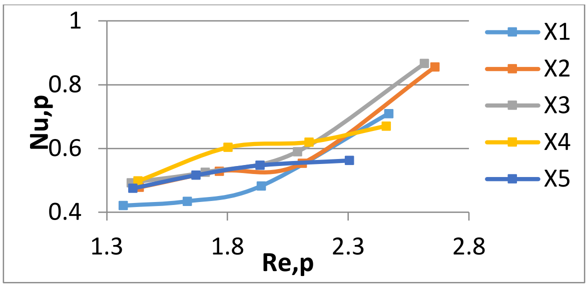

Fig. 8. Effect of Reynolds number on the particles Nusselt number for the sand samples 0.3mm

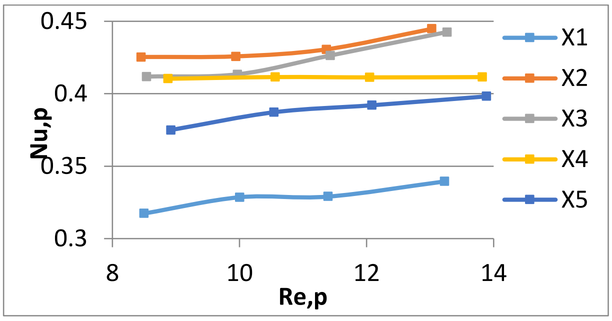

Fig. 9. Effect of Reynolds number on the particles Nusselt number for the sand samples 0.6 mm.

values of the 0.3 sand samples. It is also observed that the values of Re_p for the 0.6 mm sand sample are higher than that of 0.3 mm; furthermore, the values of Re_p for the 0.3 mm sand samples is higher than that of 0.15 mm; due to the difference in gas velocity. The diameter of sand particles which has a significant effect on the coefficient of heat transfer, since smaller particle diameter increases the coefficient of heat transfer. The heat transfer coefficient for the 0.15 mm sand particles was found to be 3.124 times higher than that of the 0.3 mm sand particles, and 6.868 times higher than that of the 0.6 mm sand particles at the same operating conditions.

4. CONCLUSION

From the discussion of results obtained from tests on the three sand samples at different hot tube locations, it was shown that the *Nu* average increases with increases in *Re* at all distances within the three sand samples due to:

1. The heat transfer coefficient which increases with increasing gas velocity.
2. The Nusselt number increases with increases in Reynolds number.
3. The effect of tube location was observed clearly since none of the tubes had the same values at different locations.

The results from the present study are compared with those obtained by Moawed [11] and had shown good agreement in terms of application, but at varying sand particle diameters.

REFERENCES

[1] Van Ommen JO, Ellis N. JMBC/OSPT course particle technology. 2010.

[2] Basu P. Combustion and gasification in fluidized beds. CRC press; 2006.

[3] Wu R, Lim C, Grace J, Brereton C. Instantaneous local heat transfer and hydrodynamics in a circulating fluidized bed. *International journal of heat and mass transfer* 1991; **34** (8): 2019-2027.

[4] Masoumifard N., Mostoufi N, Hamidi A-A, Sotudeh-Gharebagh R. Investigation of heat transfer between a horizontal tube and gas–solid fluidized bed. *International Journal of Heat and Fluid Flow*, 2008; **29** (5):1504-1511.

[5] Stefanova A, Bi H, Lim C, Grace J. Heat transfer from immersed vertical tube in a fluidized bed of group A particles near the transition to the turbulent fluidization flow regime. *International Journal of Heat and Mass Transfer* 2008; **51** (7-8): 2020-2028.

[6] Habeeb L, Al-Turaihi R. Simulation and experiment study of gas-solid flow behavior in the standpipe of a fluidized bed. *International Conference on Engineering and Information Technology*. September 2012: pp. 17-19.

[7] Yassir Makkawi, "Particle to gas heat transfer in a circulating fluidized bed riser.*10th International Conference on Circulating Fluidized Beds and Fluidization Technology-CFB-10*. T. Knowlton, PSRI Eds, ECI Symposium Series, (2013).

[8] Chourasia S, Alappat BJ. Experimental study on the attrition and size distribution of bed material in a recirculating fluidized bed. *Chemical Engineering Communications* 2017; **204**: 1174-1186.

[9] Holman JP. Heat transfer. 10th ed., New York; The McGraw Hill Companies: 2010.

[10] Moawed MA, Berbish NS, Allam AA, El-Shamy AR, M. El-Shazly K. Heat transfer between fluidized bed and horizontal bundle of tubes in a vertical channel. *International Journal of Chemical Reactor Engineering* 2010; **8** :1-28.

[11] Al-Mola YS. Experimental investigation of heat transfer from finned tube bundle immersed in shallow gas fluidized bed. MSc. Thesis: Mosul University; Mosul, Iraq: 2008

[12] Tahseen. TA. Optimal geometric arrangement of unfinned and finned flat tube heat exchanger under laminer forced convection. PhD Thesis: Universiti Malaysia Pahang; Pahang, Malasyia: 2014.

[13] Al-Dabbagh MS. The influence of air distributor on heat transfer coefficient in fluidized bed of heat pipe heat exchanger. *Al-Taqani Journal* 2005; **19** (2): 135-149.